Neuro-dynamic Control of an above Knee Prosthetic Leg

Zunaed Kibria* and Sesh Commuri†

Electrical and Biomedical Department, University of Nevada - Reno, Reno, Nevada, U.S.A.

Keywords: Neuro-dynamic Control, Prosthetic Leg, Gait Asymmetry.

Abstract: The control of a prosthetic leg for above-knee amputees is fraught with several challenges. While the dynamics of the knee-ankle system are complex and unknown, the control problem is exacerbated by the lack of desired joint trajectories as they are dictated by the locomotion needs of the individual. Improper movement of the knee and ankle joints can have serious implications for the safety of the user. Further, dissimilarities in the gait of the amputated side and the intact side can result in gait abnormalities that result in increased metabolic energy consumption and musculo-skeletal pains in the short term, and cardiovascular and other health complications in the long term. In this paper, we propose a novel neuro-dynamic control strategy that can guarantee stable control of the prosthetic limb while minimizing the gait asymmetry between the intact and prosthetic limb. Further, the algorithm learns the unknown elements of the dynamics and adapts to the changing locomotion needs of the individual. The efficacy of the proposed approach is demonstrated through numerical simulations.

1 INTRODUCTION

Above knee amputation has lasting effect on the ability of an individual to perform daily activities and can result in adverse long term consequences to the mental and physical health (Myers & Chauvin, 2021). Therefore, a proper fitting and functioning prosthetic device is essential to rehabilitate an amputee and avoid post-surgical complications such as pressure sores, arthritis, gait asymmetry and depression (Mai, 2012). In addition to providing adequate support to the individual during stance, an ideal prosthetic device should enable the individual to regain near-natural gait. To accomplish this the device must be able to ascertain the intent of the user and then generate movement of the joints to address the walking speed and the nature of terrain. Further, the response must be in real-time and should ensure the stability of the device and safety of the individual. Many of the commercially available lower limb prosthetic devices are passive, cannot adapt to changing gait requirements of the individual, and use extra metabolism energy during locomotion (Bhat et al., 2018; Versluys et al.). Computer-controlled powered prosthetic devices can address some of the requirements however, they cannot ascertain the intent of the user. Currently available powered prosthetic legs are heavy and their control mechanism is not sophisticated enough to support all daily activities (Fleming, 2021). Some researchers developed spring-based powered limbs to improve the performance of these devices (Bhat et al., 2018; Carney, 2020). But these powered limbs cannot be used for a long term as they are unable to compensate for the unknown dynamics (Carney, 2021). There are some model reference adaptive control approaches but these approaches are based on linearized model and their performance deteriorates rapidly outside a small region of operation (Pagel, 2017).

Several companies such as Ossur, Ottobock, SpringActive, BionX Medical Technologies, Freedom Innovations etc., have commercialized active powered limbs (Windrich, 2016). Though these devices provide good performance in terms of locomotion, they use traditional control techniques based on linear approximations of the system and are unable to compensate for unmodeled dynamics. Further, the control parameters of these devices have to be adjusted to address the requiremnents of each individual. Several researchers explored the use of neural networks and reinforcement learning to control artificial knee and ankle joint with varying degrees of

---

* https://www.linkedin.com/in/zunaed-kibria-984743107/
† https://www.unr.edu/ebme/people/sesh-commuri

success (Mai & Commuri, 2016; Stolyarov, 2021; Wen, 2017). However, these approaches ignore the coupled dynamics between the knee and the ankle thereby limiting the performance of these devices.

While the primary function of a lower-limb prothesis is to provide support during stance, the ability to provide near-natural gait is essential to the long-term health of the individual. Asymmetric gait can cause individuals to expend more metabolic energy (Ryan et al., 2020). Asymmetric gait can also lead to serious long-term injuries and poor quality of life (Pirker, 2017). Impaired gait in the elderly can lead to dementia and other neurological diseases (Mielke et al., 2012). Therefore, it is desirable for a prosthetic device to reduce gait asymmetry between the intact and amputated side of an individual.

Design of a control system for above-knee prosthesis is difficult for following reasons:

- Ideal joint displacement profiles cannot be specified prior to locomotion because it depends on the intent of the indivisual.
- During a gait cycle the knee and ankle joints are affected by dynamical coupling of the prosthetic leg system and residual hip.
- Ground reaction force is proportional to the body weight of a person and provides the necessary propulsion for the gait (Perry, 2010). While walking, lower limb joints are influenced by ground reaction force which in turn affects the knee and ankle joints in the form of disturbance torque. Uncompensated disturbaces will degrade the performance of the controller.

Neuro-dynamic programming (NDP) has shown promising results in the control of uncertain complex dynamical systems (Bugeja, 2008; Lu et al., 2008; Mahmud et al., 2021). NDP is based on approximation theory and neural networks and uses Bellman's optimality principle to improve the control decision at each step to result in lower long term cost (Bertsekas, 1995). However, traditional optimal control had limited success in the control of prosthetic leg (Chen et al., 2020; Rigatos, 2017).

In this paper, we implement a neuro-dynamic control approach for above-knee prosthetic system to reduce gait asymmetry and achieve near natural gait. The controller action is two-fold: At a lower level, a filtered tracking error system ensures that the joints follow the prescribed dipslacement profile. At a higher level, the Critic Network computes the "to go" cost and modifies the control action to minimize the long-term cost. As a result, the performance of the controller improves after each step, i.e., after each stance phase of the gait. For this approach to be successful, desired displacement profiles for the knee and the ankle are first selected using gait information from the intact side of the individual. A filtered tracking error system generates the control torque that enables the knee and ankle joints to track the prescribed trajectories. A neural network is used to learn the unknown dynamics of the system. After each stance phase the "look ahead" costs are computed and the wieghts of the critic network are updated to minimize the costs. Simulation results demonstrate that the knee and ankle joints as well as the angle the foot makes with the ground track the corresponding profiles on the intact side, thereby improving stance and reducing assymetry.

The rest of the paper is organized as follows - a dynamical model of the prosthetic system is developed in section 2. In section 3, the modeling of kinematic profiles and ground reaction force is described. The design and detailed formulations of the proposed controller are provided in section 4. The stability of the proposed approach and the efficacy in reducing gait assymetry is demonstrated through simulation results in section 5. Conclusions of the proposed technique and scope of future work are discussed in section 6.

2 DYNAMICAL MODEL

In this study, we examine the dynamics of a transfemoral prosthesis used to improve the mobility of an above knee amputee. The prosthetic device comprises of a knee joint and an ankle joint connected to the residual limb through a snug socket (Figure 1). While the dynamics of such a device are complex, we consider a simplified link segment representation of residual limb (Figure 1) that captures the movement in the sagittal plane (Mai & Commuri, 2016):

$$M_{ka}(\theta)\ddot{\theta} + V_{ka}(\theta,\dot{\theta})\dot{\theta} + G_{ka}(\theta) + F_{ka}(\dot{\theta}) + \tau_d = \tau + \tau_G \quad (1)$$

where, $'M_{ka}(\theta)'$ denotes the inertia matrix of the coupled dynamics representing the knee-ankle system, $'V_{ka}(\theta,\dot{\theta})'$ stands for the Coriolis/ centripetal matrix, $'G_{ka}(\theta)'$ stands for the gravitational vector, $'F_{ka}(\dot{\theta})'$ represents the frictional terms, $'\tau_d'$ represents the disturbance torque. On the right side of equation (1), $'\tau'$ is a 2x1 dimensional vector that represents the torque generated by each joint and $'\tau_G'$ represents the ground reaction torque. $'\theta'$ and $'\dot{\theta}'$ are vector quantities that represent joint angles and angular velocities. $'\ddot{\theta}'$ represents angular acceleration.

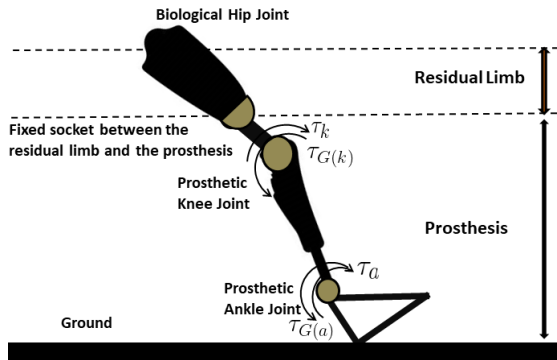The details of the matrices in equation (1) are given in the Appendix.

Figure 1: Link segment representation of the prosthetic leg. Subscripts 'k' and 'a' denote quantities corresponding to knee joint and ankle joint respectively.

3 KINEMATIC PROFILES AND GROUND REACTION TORQUE

The inability to properly coordinate the movement of the knee and ankle joints during locomotion can lead to several musculoskeletal and neurological disorders over time (Ranavolo, 2012). Therefore, the knee and ankle joints of a prosthetic leg must function in coordination to ensure the long-term health of the individual. Further, the position of the foot during gait is related to the instantaneous displacement of these joints. The movement of the prosthetic foot has to be nearly identical to that of the intact foot during corresponding instants in gait in order to reduce the asymmetry between the intact and amputated sides of the individual.

The first step in the design of a controller is to determine the desired displacement profiles for the knee and ankle joints. This is problematic as these displacement profiles are dependent on the intent of the user and the terrain and are unknown at the time of control. For example, walking at slow pace versus walking at a brisk pace results in different displacement profiles of these two joints.

In this paper we explore the use of nominal gait profiles that can be parameterized and used to study the gait of an individual over a variety of walking speeds. Considering the knee and ankle joints of an individual as shown in Figure 2, the nominal gait profile can be studied by dividing the gait into stance and swing phases (Figure 3). In the stance phase, the foot is in contact with the ground and supports the weight of the body. As the foot progresses from the stance to the swing phase, the weight of the body is
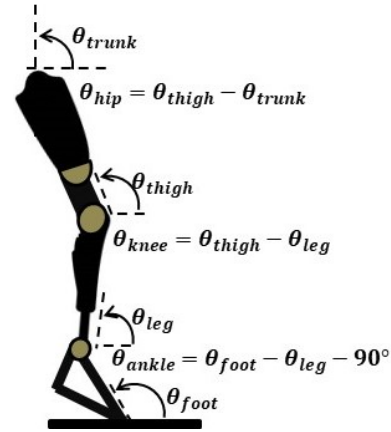

Figure 2: Prosthetic leg joints angles.

transferred to the other foot. The stance phase starts with 'Heel Strike' when the foot comes in contact with the ground. As the stance progresses to 'Foot flat' and 'Mid stance' subphases, more of the body weight is supported by the foot. After 'Heel-Off' and 'Toe-Off' subphases the leg enters into the swing phase and the body weight shifts to the opposite leg. The nominal gait profiles for knee and ankle joints and foot position relative to the ground is given in Figure 3.
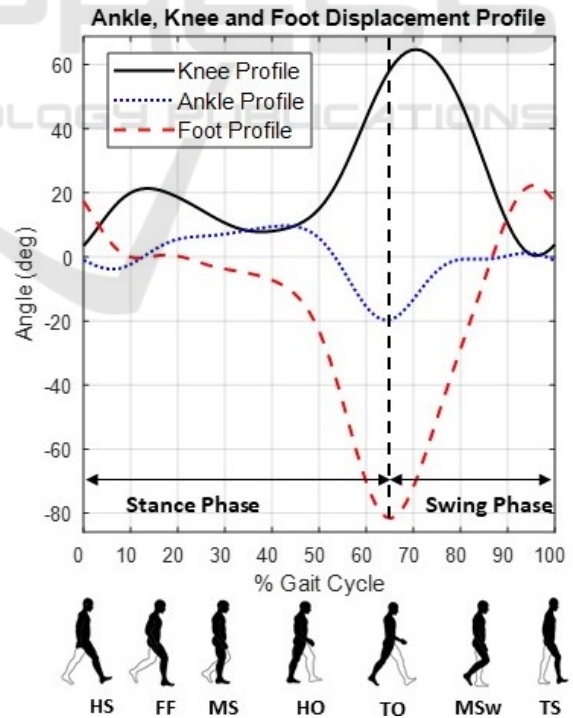

Figure 3: Nominal gait profiles for knee, ankle joints and foot position relative to the ground; HS = Heel Strike, FF= Foot Flat, MS = Mid Swing, HO = Heel off, TO = Toe Off, MSW = Mid Swing, TS = Terminal Swing.

Ground reaction torques acting on the leg joints are a direct consequence of ground reaction force. Ground reaction force (GRF) is the counter force of the ground to human body during a gait. Ground reaction force (GRF) is proportional to body weight and transferred up to the leg joints and results in proportional torques. To maintain a stable forward dynamics during a gait, ground reaction force needs to be accounted as an external force acting on the system (Peasgood et al., 2006). GRF is typically evaluated in a loboratory setting using force plates. It is difficult to measure GRF outside a motion laboratory because of the lack of force plates to measure GRF (Recinos et al., 2020). In this paper, we estimate the ground reaction force and torque into the knee and ankle joints with following equations (Millard, 2008):

$$F_z = \bar{k}(z_P)^{spe} + Step(y, 0, 0, d_{max}, c_{max})\dot{z}_p$$
$$F_x = \bar{\mu} \, F_z \, sgn(v_{xcop}) \qquad (2)$$
$$\tau_G = d_z F_x + d_x F_z$$

where, the vertical and horizontal force components on the joints are denoted as $'F_z'$ and $'F_x'$. $'z_P'$ and $'\dot{z}_p'$ are penetration and penetration rate of the foot, '$\bar{k}$', '$\bar{\mu}$', 'spe' are spring coefficient, friction coefficient and spring exponent. $'d_{max}'$, $'c_{max}'$ are maximal damping penetration and maximal damping coefficient. 'v_{xcop}' is the horizontal velocity of the contact point relative to the ground. 'τ_G' stands for the ground reaction torque. 'd_z' and 'd_x' are the vertical and horizontal distances of the joints with respect to the foot-ground contact point.

To develop a control system to generate appropriate torque for the knee and ankle joints, we parameterize the nominal gait profiles and ground reaction torques. Gait profiles and ground reaction torques are approximated with following Fourier equations:

$$\theta(t) = a_0 + \sum_{n=1}^{5}(a_n \cos \omega t + b_n \sin \omega t) \qquad (3)$$

$$\tau_G(t) = c_0 + \sum_{n=1}^{5}(c_n \cos \omega t + d_n \sin \omega t) \qquad (4)$$

where, $'\omega'$ is the angular velocity of the joint angles at 't' instance. $'a_0'$, $'c_0'$, $'a_n'$, $'b_n'$, $'c_n'$, $'d_n'$ can be found out using curve fitting algorithm (Mai, 2013).

4 CONTROLLER DESIGN

To design a controller to track the gait profiles shown in Figure 3, we first define the tracking error vector 'e' and its derivative 'ė' as follows:

$$e = (\theta_r - \theta)$$
$$\dot{e} = (\dot{\theta}_r - \dot{\theta}) \qquad (5)$$

where, $\theta_r = [\theta_{rk} \quad \theta_{ra}]^T$; $\dot{\theta}_r = [\dot{\theta}_{rk} \quad \dot{\theta}_{ra}]^T$; $'\theta_{rk}'$, $'\theta_{ra}'$, $'\dot{\theta}_{rk}'$, $'\dot{\theta}_{ra}'$ are desired angular positions and velocities for knee and ankle joints. The dynsmics of the system in equation (1) can be represented using the filtered tracking error 'r' as

$$r = \dot{e} + \lambda e \qquad (6)$$

where, r is a 2x1 dimensional vector and $\lambda > 0$ is a design parameter. Using equation (5), we can represent the dynamics of the prosthetic system (1) as

$$M_{ka}\dot{r} = -V_{ka}r + f(x) - \tau \qquad (7)$$

where, $f(x)$ comprises the nonlinear terms of the system.

$$f(x) = M_{ka}(\ddot{\theta}_r + \lambda \dot{e}) + V_{ka}(\dot{\theta}_r + \lambda e) + F_{ka} + G_{ka} - \tau_G + \tau_d \qquad (8)$$

To estimate the nonlinear terms of the system, we propose a neuro-dynamic control structure that will learn the unknown dynamics of the system and generate control input 'τ' that is applied to knee and ankle joints to achieve a smooth gait and minimize the long-term cost function. The control input to the system is designed as:

$$\tau = \hat{f}(x) + K_v r - \upsilon \qquad (9)$$

where, $\hat{f}(x)$ is the estimation of f(x), K_v is design parameter, r is the filtered tracking error, $\upsilon = -\acute{\upsilon}sgn(r)$ is a robustifying term.

To design the proposed controller, heel strike (HS) to heel strike (HS) instances have been considered as one gait cycle. During one cycle, in each instance we have defined the short-term costs for knee joint and ankle joints as a function of their tracking errors. The short-term cost function of the prosthetic system is defined as $S(t)$. $S(t)$ is a 2x1 dimensional vector comprises knee and ankle joints' cost functions S_k and S_a.

$$S(t) = [S_k \quad S_a]^T$$

$$S_k(t) = -\frac{1}{2}(\frac{\theta_{rk} - \theta_k}{\theta_{mk}})^2 - \frac{1}{2}(\frac{\dot\theta_{rk} - \dot\theta_k}{\dot\theta_{mk}})^2 \quad (10)$$

$$S_a(t) = -\frac{1}{2}(\frac{\theta_{ra} - \theta_a}{\theta_{ma}})^2 - \frac{1}{2}(\frac{\dot\theta_{ra} - \dot\theta_a}{\dot\theta_{ma}})^2$$

where $\theta_{rk}, \theta_{ra}, \dot\theta_{rk}, \dot\theta_{ra}$ are desired angular positions and velocities for knee and ankle joints. $\theta_k, \theta_a, \dot\theta_k, \dot\theta_a$ are actual angular positions and velocities for knee and ankle joints. $\theta_{mk}, \theta_{ma}, \dot\theta_{mk}, \dot\theta_{ma}$ are the maximal values for position and velocities for knee and ankle joints.

To analyze the prolonged effect of the proposed controller, the long-term cost of the system is caluclated. Long term cost is defined as the accumulated cost of the short time costs in equation (10). Long term cost function for prosthetic system can be represented as:

$$L(t) = S(t + 1) + \alpha S(t + 2) + \\ \alpha^2 S(t + 3) + \cdots \quad (11) \\ = S(t + 1) + \alpha L(t + 1)$$

In which, α $(0 < \alpha < 1)$, is a discount factor and S(t) is the short-term cost function.

The critic network generates 'J(t)' as an approximation of the long-term cost function 'L(t)'. Approximation of long-term cost function is defined with an RBF NN:

$$h_{c(j)} = exp^{-\frac{|x_c - \mu_j|}{b_j}} \; ; j = 1,2,3,4, \dots k \quad (12) \\ J(t) = W_c{}^T h_c(x_c) + \varepsilon$$

where 'x_c' is the input to the network. $'\mu_j'$, $'b_j'$ is the center and width of the gaussian of the neural net 'k'. 'W_c' represents the weight of the critic network and $'\varepsilon'$ is a very small value.

In this control structure, critic network inputs are:

$$x_c = [e_k \; e_a \; \dot e_k \; \dot e_a \; \theta_k \; \theta_a \; \dot\theta_k \; \dot\theta_a \; \hat f_k(x_{Ac}) \; \hat f_a(x_{Ac})] \quad (13)$$

In which, $e_k, e_a, \dot e_k, \dot e_a$ are knee and ankle joints' tracking errors and their derivatives. $\theta_k \; \theta_a \; \dot\theta_k \; \dot\theta_a$ are knee and ankle joints' calculated angles and velocities. $\hat f_k(x_{Ac}), \hat f_a(x_{Ac})$ are non-linearities estimation of knee and ankle joints by actor network. Approximation of the non linearities is defined by RBF NN:

$$h_{Ac(j)} = exp^{-\frac{|x_{Ac} - \mu_j|}{b_j}} \; ; j = 1,2,3,4, \dots k \quad (14) \\ f(x_{Ac}) = W_a{}^T h_{Ac}(x_{Ac}) + \varepsilon$$

where 'x_{Ac}' is the input to the actor network. $'\mu_j'$, $'b_j'$ is the center and width of the gaussian of the neural net 'k'. 'W_a' represents the weight of the actor network and $'\varepsilon'$ is a very small value.

The backpropagation error for critic network $'e_c'$ is defined as:

$$e_c = [J(t - 1) - S(t)] - \alpha J(t) \quad (15)$$

Update laws of the critic network are defined as:

$$\dot W_c = \alpha F h_c r^T - \kappa F \|e_c\| W_c \quad (16)$$

where 'α' is the discount factor, and 'F' and $'\kappa'$ are design parameters. 'r', 'e_c' are filtered tracking error and critic network's backpropagation error respectively. Further, 'h_c' for critic network can be computed using (12).
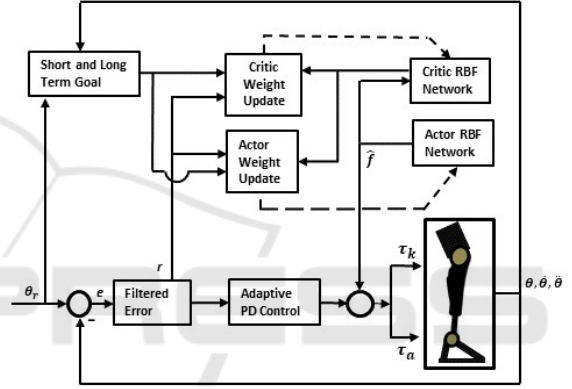

Figure 4: NDP Control Structure for prosthetic leg.

With the help of the critic network, the actor network updates itself to reduce the long-term cost and approximate the nonlinearities of knee and ankle joints. By learning the nonlinearities of the system, it exerts proper torque to the knee and ankle joints for smooth locomotion. To learn and estimate the non-linearities with the actor network we use RBF network mentioned in equation (12). Input to the actor network are:

$$x_{Ac} = [e_k \; e_a \; \dot e_k \; \dot e_a \; \theta_k \; \theta_a \; \dot\theta_k \; \dot\theta_a \; \ddot\theta_k \; \ddot\theta_a] \quad (17)$$

Where, $e_k, e_a, \dot e_k, \dot e_a$ are knee and ankle joints' tracking errors and their derivatives. $\theta_k, \theta_a, \dot\theta_k, \dot\theta_a, \ddot\theta_k, \ddot\theta_a$ are knee and ankle joints' calculated angles, velocities and accelerations.

The input law into the system is corrected by the actor network to minimize the long-term cost function. In order to find out a control goal which reduce the infinite horizon long term system cost to minimum possible value, we define an ultimate control goal '$U_c(t)$'. The ultimate control goal '$U_c(t)$'

33

= 0, which is the long-term cost approximation of 'J(t)'.

Back propagation error for actor network is given as follows:

$$e_{Ac} = U_c(t) - J(t) \qquad (18)$$

The tuning rule for actor network is given as:

$$\dot{W}_a = Fh_{Ac}r^T - \kappa F\|e_{Ac}\|W_a \qquad (19)$$

In which, 'F' and 'κ' are design parameters. 'r', 'e_{Ac}' are filtered tracking error and actor network's backpropagation error respectively. 'h_{Ac}' for actor network can be computed using (14).

Theorem: The control law in equation (9) with the actor and critic network weight update laws in equation (16) and (19), ensures the tracking errors in equation (5) will be ultimately bounded. Further, the cumulative long-term cost will be bounded.

5 NUMERICAL EXAMPLE

In this section simulation results have been provided to demonstrate proposed controller's performance. These simulation experiments were designed to study the performance with respect to:

a) tracking the desired knee and ankle joint profiles,

b) estimation of the nonlinear terms in the dynamics,

c) orientation of the foot relative to the ground during a gait,

d) adaptability to variable walking speed, and

e) robustness to measurement and actuator noises.

5.1 Experimental Setup

In order to study the performance of the proposed control strategy, it is assumed that the prosthetic device is fitted on a healthy male of height 1.78 meters and weighing 90.7 kilograms. Corresponding gait data from a similar intact individual is first collected and analyzed. In these simulation studies it is assumed that the individual is walking in normal cadence. Based on the cadence, nominal trajectories for knee and ankle joints are then approximated using parameterization of nominal gait data collected from human subjects (Winter 2009). From Figure 5, it can be seen that the approximate displacement profile for the knee is close to the actual knee profile of an individual.
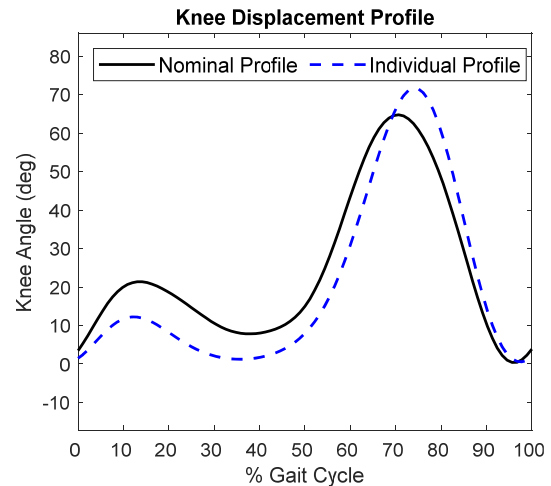

Figure 5: Nominal and individual's knee displacement profiles.

Further, data in Table 1 shows that at each phase of the gait, the approximate displacement profile is within a small bound of the actual displacement profile seen in a similar intact individual. Therefore, in these simulation examples, the stance time is first measured from the intact side and then used to generate a desired displacement profiles using the parametrization of naminal gait.

Table 1: Knee, Ankle and Foot angles for nominal and individual's gait profiles during stance phase. Nom. = Nominal, Ind. = Individual. HS=Heel Strike, FF = Foot Flat, MS = Mid Stance, HO = Heel Off, TO = Toe Off.

Gait Ph.	Knee Angle		Ankle Angle		Foot Angle	
	Nom.	Ind.	Nom.	Ind.	Nom.	Ind.
HS	3.48	1.47	-1.00	-4.67	17.35	7.68
FF	19.68	11.61	-2.46	1.64	0.00	1.05
MS	14.63	4.47	6.43	6.43	0.58	-1.09
HO	9.04	2.85	9.70	12.11	-9.99	-4.18
TO	58.39	62.69	-15.94	-6.84	-81.60	-71.19

5.2 Simulation Results

The parameters for model dynamics and design values are given in the Appendix (Table 4-5). The tracking performance of the knee and ankle joints and foot position is shown in Figures (6-8). Figure 6 shows that the proposed NDP controller is able to track the nominal knee and ankle profiles with very little error. Actor network is able to accurately estimate the non-linearities associate with knee and ankle joints (Figure 7). As a result, the foot position is maintained close to the desired position during different gait phases. It is observed in Figure 8 that the foot position in both stance and swing phase of the

prosthesis is similar to that of an intact leg. Further during the Foot Flat (FF) to Mid Stance (MS) phase, the controller is able to maintain desired foot position identical to an intact leg. This implies that the stance on both intact and prosthetic side is similar leading to the conclusion that the weight bearing is similar on both sides.
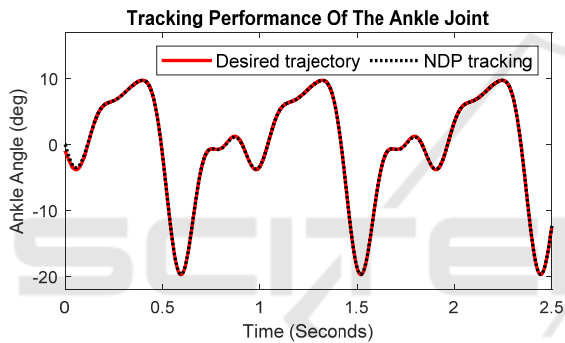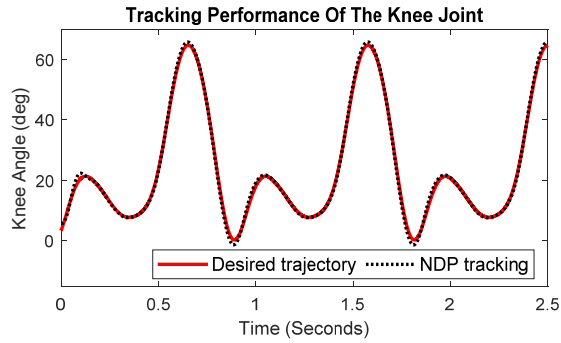

Figure 6: Tracking performance of NDP for knee and ankle joints.
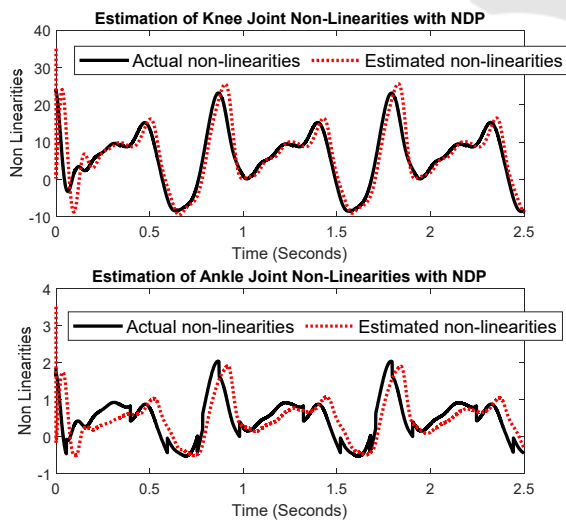

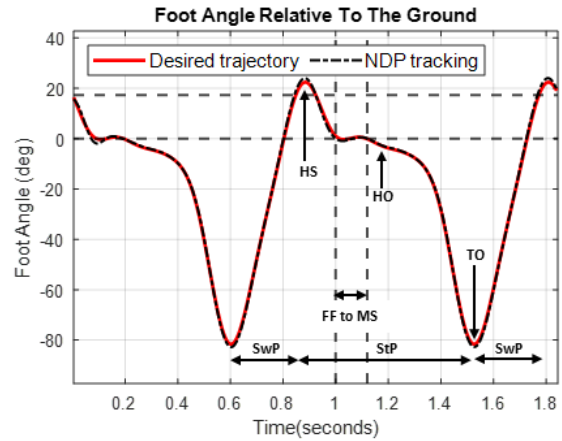Figure 7: Estimation of Nonlinearities for knee and ankle joint.

Figure 8: Foot position of the prosthetic leg with NDP controller. (HS=Heel Strike, FF = Foot Flat, MS = Mid Stance, HO = Heel Off, TO = Toe Off, SwP = Swing Phase, StP = Stance Phase).

To check the effect of variations in walking speed, we calculate the long-term costs associated with knee and ankle joints with the proposed control model. We have tabulated the long-term cost for 3 steps with medium, slow and fast cadence (Table 2). To compare the proposed controller's performance with traditional PD and adaptive NN based controllers we perform simulation with same set up and observe that NDP based controller outperforms both PD and Adaptive NN controllers (Table 2).

Table 2: Long-term cost for different walking cadence.

Gait Type	Joint	PD	Adaptive NN	NDP
Medium Cadence	Ankle joint	1.05	0.4694	0.0082
	Knee joint	5.05	1.3513	0.0083
Slow Cadence	Ankle joint	0.65	0.3728	0.0055
	Knee joint	5.59	0.9657	0.0055
Fast Cadence	Ankle joint	1.8698	0.6981	0.0984
	Knee joint	6.0650	2.0096	0. 0985

To investigate the performance of the proposed controller with noise, uniformly distributed measurement and actuator noises are added into the system. System is affected with 2% added measurement noise to θ and $\dot{\theta}$ and 20% actuator noise to τ. Considering the individual is walking in a medium cadence, we analyze the long-term cost for the proposed NDP, PD and Adaptive NN controllers in noisy environment. It is observed from the simulation results tabulated in Table 3 that NDP based controller is less susceptible to added noise and performs better than the rest controllers in terms of long-term cost.

Table 3: Long term cost with increasing measurement and actuator noise.

Noise	Joint	PD	Adaptive NN	NDP
2% measurement Noise	Ankle joint	1.34	0.4845	0.0227
	Knee joint	5.5678	1.3868	0.0127
20% actuator noise	Ankle joint	1.2686	0.4917	0.0241
	Knee joint	5.2235	1.1219	0.0242

6 CONCLUSIONS

In this paper, a novel neuro-dynamic control approach for above-knee prosthetic system was developed to reduce gait asymmetry and achieve near natural gait. Using a filtered tracking error system and an actor-critic network, the controller was shown to be able to track synthesised displacement profiles for the knee and ankle joints while reducing the long-term cost. As a result, the performance of the controller improves after each step, i.e., after each stance phase of the gait. Data collected in the lab indicates that the synthesised gait profiles are close to the knee and ankle displacements in an intact individual while walking at self-selected pace. Simulation results demonstrate that the knee and ankle joints as well as the angle the foot makes with the ground track the corresponding profiles on the intact side, thereby improving stance and reducing assymetry. In the future, the performance of the controller will be verified on a prosthetic device mounted on a gait simulator.

REFERENCES

Bertsekas, D. P. a. T. J. N. (1995). *Neuro-dynamic programming : an overview* Proceedings of 1995 34th IEEE Conference on Decision and Control, New Orleans, LA, USA.

Bhat, S. G., Redkar, S., & Sugar, T. G. (2018). Development of a Passive Prosthetic Ankle With Slope Adapting Capabilities. ASME 2018 International Mechanical Engineering Congress and Exposition, Bugeja, M. K. a. F. S. G. (2008). *Neuro-adaptive dynamic control for mobile robots: Experimental validation* 2008 3rd International Symposium on Communications, Control and Signal Processing, Saint Julian's, Malta.

Carney, M. E. a. H. H. (2020). *Electric-Energetic Consequences of Springs in Lower-Extremity Powered Prostheses on Varied Terrain* 2020 8th IEEE RAS/EMBS International Conference for Biomedical Robotics and Biomechatronics (BioRob), New York, NY, USA. 10.1109/BioRob49111.2020.9224458

Carney, M. E. a. S. T. a. S. R. a. D. J.-F. a. H. H. M. (2021). Design and Preliminary Results of a Reaction Force Series Elastic Actuator for Bionic Knee and Ankle Prostheses. *IEEE Transactions on Medical Robotics and Bionics*, *3*(3), 542-553. https://doi.org/10.1109/TMRB.2021.3098921

Chen, T., Babanin, A., Muhammad, A., Chapron, B., & Chen, C. (2020). Modified Evolved Bat Algorithm of Fuzzy Optimal Control for Complex Nonlinear Systems. *Romanian Journal Of Information Science And Technology*, *23*, 28-40.

Fleming, A. a. H. S. a. B. E. a. H. F. a. H. H. H. (2021). Direct continuous electromyographic control of a powered prosthetic ankle for improved postural control after guided physical training: A case study. *Wearable Technologies*, *2*, e3. https://doi.org/10.1017/wtc.2021.2

Lu, C., Si, J., & Xie, X. (2008). Direct heuristic dynamic programming for damping oscillations in a large power system. *IEEE Transactions on Systems, Man, and Cybernetics, Part B: Cybernetics*, *38*(4 ,), 1008--1013. https://doi.org/10.1109/TSMCB.2008.923157

Mahmud, S. M. N., Nivison, S. A., Bell, Z. I., & Kamalapurkar, R. (2021). Safe Model-Based Reinforcement Learning for Systems With Parametric Uncertainties [Original Research]. *Frontiers in Robotics and AI*, *8*. https://doi.org/10.3389/frobt.2021.733104

Mai, A., & Commuri, S. (2016). Intelligent control of a prosthetic ankle joint using gait recognition. *Control Engineering Practice*, *49*, 1-13. https://doi.org/10.1016/j.conengprac.2016.01.004

Mai, A. a. C. S. (2013). *Intelligent Control of a Prosthetic Ankle Joint* International Conference on Informatics in Control, Automation and Robotics, https://www.scitepress.org/Papers/2013/44856/pdf/index.html

Mai, A. a. C. S. a. D. C. P. a. D. J. a. E. W. J. J. a. R. J. L. (2012). Effect of Prosthetic Foot on Residuum-Socket Interface Pressure and Gait Characteristics in an Otherwise Healthy Man With Transtibial Osteomyoplastic Amputation. *JPO: Journal of Prosthetics and Orthotics*, *24*(4).

Mielke, M. M., Roberts, R. O., Savica, R., Cha, R., Drubach, D. I., Christianson, T., Petersen, R. C. (2012). Assessing the Temporal Relationship Between Cognition and Gait: Slow Gait Predicts Cognitive Decline in the Mayo Clinic Study of Aging. *The Journals of Gerontology: Series A*, *68*(8), 929-937. https://doi.org/10.1093/gerona/gls256

Millard, M. a. M. J. a. K. E. (2008). *Multi-Step Forward Dynamic Gait Simulation* (Vol. 12). https://doi.org/10.1007/978-1-4020-8829-2_2

Myers, M., & Chauvin, B. (2021). Above the Knee Amputations. In. Florida: StatPearls Publishing.

P. (1996). Adjustments to Zatsiorsky-Seluyanov's segment inertia parameters. *Journal of Biomechanics*, *29*(9), 1223-1230. https://doi.org/https://doi.org/10.1016/0021-9290(95)00178-6

Pagel, A. a. R. R. a. R. R. a. V. H. (2017). Bio-Inspired Adaptive Control for Active Knee Exoprosthetics. *IEEE Transactions on Neural Systems and Rehabilitation Engineering*, *25*(12), 2355-2364. https://doi.org/10.1109/TNSRE.2017.2744987

Peasgood, M., Kubica, E., & McPhee, J. (2006). Stabilization of a Dynamic Walking Gait Simulation. *Journal of Computational and Nonlinear Dynamics*, *2*(1), 65-72. https://doi.org/10.1115/1.2389230

Perry, J. (2010). Gait Analysis: Normal and Pathological Function. *Journal of Sports Science \& Medicine*, *9*(2), 353-353.

Pirker, W. a. K. R. (2017). Gait disorders in adults and the elderly. *Wiener klinische Wochenschrift*, *129*(3), 81-95. https://doi.org/10.1007/s00508-016-1096-4

Ranavolo, A. a. D. L. M. a. M. S. a. S. M. a. S. A. a. I. S. a. C. E. a. A. R. a. P. A. (2012). Lower-Limb Joint Coordination Pattern in Obese Subjects. *BioMed Research International*.

Recinos, E., Abella, J., Riyaz, S., & Demircan, E. (2020). Real-Time Vertical Ground Reaction Force Estimation in a Unified Simulation Framework Using Inertial Measurement Unit Sensors. *Robotics*, *9*(4), 88.

Rigatos, G. a. S. P. a. S. D. a. P. R. E. (2017). Nonlinear Optimal Control of Oxygen and Carbon Dioxide Levels in Blood. *Intelligent Industrial Systems*, *3*(2), 61-75. https://doi.org/10.1007/s40903-016-0060-y

Ryan, H. P., Husted, C., & Lewek, M. D. (2020). Improving Spatiotemporal Gait Asymmetry Has Limited Functional Benefit for Individuals Poststroke. *Journal of Neurologic Physical Therapy*, *44*(3), 197-204. https://doi.org/10.1097/npt.0000000000000321

Stolyarov, R. a. C. M. a. H. H. (2021). Accurate Heuristic Terrain Prediction in Powered Lower-Limb Prostheses Using Onboard Sensors. *IEEE Transactions on Biomedical Engineering*, *68*(2), 384-392. https://doi.org/10.1109/TBME.2020.2994152

Versluys, R., Beyl, P., Damme, M. V., Desomer, A., Ham, R. V., & Dirk, L. (2009). Prosthetic feet: State-of-the-art review and the importance of mimicking human ankle–foot biomechanics. *Disability and Rehabilitation: Assistive Technology*, *4*(2), 65-75 , year = 2009. https://doi.org/10.1080/17483100802715092

Wen, Y. a. S. J. a. G. X. a. H. S. a. H. H. H. (2017). A New Powered Lower Limb Prosthesis Control Framework Based on Adaptive Dynamic Programming. *IEEE Transactions on Neural Networks and Learning Systems*, *28*(9), 2215-2220. https://doi.org/10.1109/TNNLS.2016.2584559

Windrich, M. a. G. M. a. C. O. a. R. S. a. B. P. (2016). Active lower limb prosthetics: a systematic review of design issues and solutions. *BioMedical Engineering OnLine*, *15*(3), 140. https://doi.org/10.1186/s12938-016-0284-9

APPENDIX

Dynamics Matrices: $M_{ka}(\theta) = \begin{bmatrix} M_{ka(1,1)} & M_{ka(1,2)} \\ M_{ka(2,1)} & M_{ka(2,2)} \end{bmatrix}$

$$M_{ka(1,1)} = (m_k + m_a)l_k^2 + m_a l_a^2 + 2m_a l_k l_a \cos\theta_a$$

$$M_{ka(1,2)} = M_{ka(2,1)} = m_a l_a^2 + m_a l_k l_a \cos\theta_a$$

$$M_{ka(2,2)} = m_a l_a^2$$

$$V_{ka}(\theta,\dot{\theta}) = \begin{bmatrix} -m_a l_k l_a(2\dot{\theta}_k\dot{\theta}_a + \dot{\theta}_a^2)\sin\theta_a \\ m_a l_k l_a \dot{\theta}_k^2 \sin\theta_a \end{bmatrix}$$

$$G_{ka}(\theta) = \begin{bmatrix} (m_k + m_a)gl_k\cos\theta_k + m_a gl_a\cos(\theta_k + \theta_a) \\ m_a gl_k\cos(\theta_k + \theta_a) \end{bmatrix}$$

$$F_{ka}(\theta) = \kappa_{d(\theta)}sgn(\dot{\theta})$$

$$\theta = [\theta_k \quad \theta_a]^T; \dot{\theta} = [\dot{\theta}_k \quad \dot{\theta}_a]^T; \ddot{\theta} = [\ddot{\theta}_k \quad \ddot{\theta}_a]^T.$$

$$\tau_d = [\tau_k \quad \tau_a]^T; \tau_G = [\tau_{G(k)} \quad \tau_{G(a)}]^T; \tau = [\tau_k \quad \tau_a]^T$$

Subscripts 'k' and 'a' denotes knee and ankle joints respectively.

Table 4: Plant parameters.

m_k (*Knee to ankle link (Shank) mass*)	3.16 kg
m_a (*Ankle and foot mass*)	1.001 kg
l_k (*Knee to ankle joint length*)	0.07 m
l_a (*Ankle joint to heel length*)	0.093 m
g (*Gravitational acceleration*)	9.8 ms-2
$\kappa_{d(\theta)}$ (*Dynamic Friction Coefficient*)	0.2

Assuming that the individual is an average male weighing 73.0 kilograms (kgs) and of height 1.741 meters (m), m_k, m_a, l_k, l_a are collected from (P, 1996)

Table 5: Design values.

λ(*Design parameter*)	6
K_v(*Design parameter*)	4
$\acute{\upsilon}$(*Design Parameter*)	0.3
α (*Discount factor*)	0.95
F (NN tuning gain)	$\begin{bmatrix} 22 & 0 \\ 0 & 22 \end{bmatrix}$
κ (NN design parameter)	1
$\bar{k}$ (Spring coefficient to measure GRF)	2×10^6 Nm^{-1}
Spe (Spring exponent to measure GRF)	2.2
$\bar{\mu}$ (Friction coefficient to measure GRF)	0.2
Network structure for actor and critic	Input node: 10 Hidden layer: 30 Output layer: 2